

The impact of Yb³⁺ concentration on multiband upconversion in single NaYF₄:Yb/Er microcrystal determined via nanosecond time-resolved spectroscopy

Hanchang Huang,^{a,‡} Maohui Yuan,^{a,‡} Zhongyang Xing,^{a,‡} Wenda Cui,^{a,b} Tongcheng Yu,^{a,b} Shuai Hu,^a

Guomin Zhao,^{a,b} Chuan Guo,^{*,a,b} and Kai Han^{*,a,c}

^aCollege of Advanced Interdisciplinary Studies, National University of Defense Technology, Changsha, 410073, China. E-mail: guochuan20@nudt.edu.cn, hankai0071@nudt.edu.cn.

^bHunan Provincial Key Laboratory of High Energy Laser Technology, Changsha, 410073, China.

^cState Key Laboratory of Pulsed Power Laser Technology, Changsha, 410073, China.

[‡]These authors contributed equally to this work and should be considered co-first authors.

Although multi-band emissions of β-NaYF₄:Yb³⁺/Er³⁺ can be observed from single MCs under ns-pulsed excitation at high power density, the emissions are concentrated on some wavelengths (such as 654, 542, 522 and 410 nm) in terms of the total UCL produced by each pulse excitation. Figure S1 shows the power-dependent UCL spectra under the excitation of pulsed laser. The slope of the fitting curve reveals the power efficiency for UCL, which is based on the formula of $I_{UCL} \propto P^n$ (where, I_{UCL} represents luminescence intensity, P represents power, n represents the number requirement of photons).¹ According to the power-dependent curve of ns-pulsed excitation, it can be concluded that the UCL increases with the pulsed laser energy. With increasing the Yb³⁺ doping concentrations, the UCL quenching effect is enhanced and the power efficiency decreases.

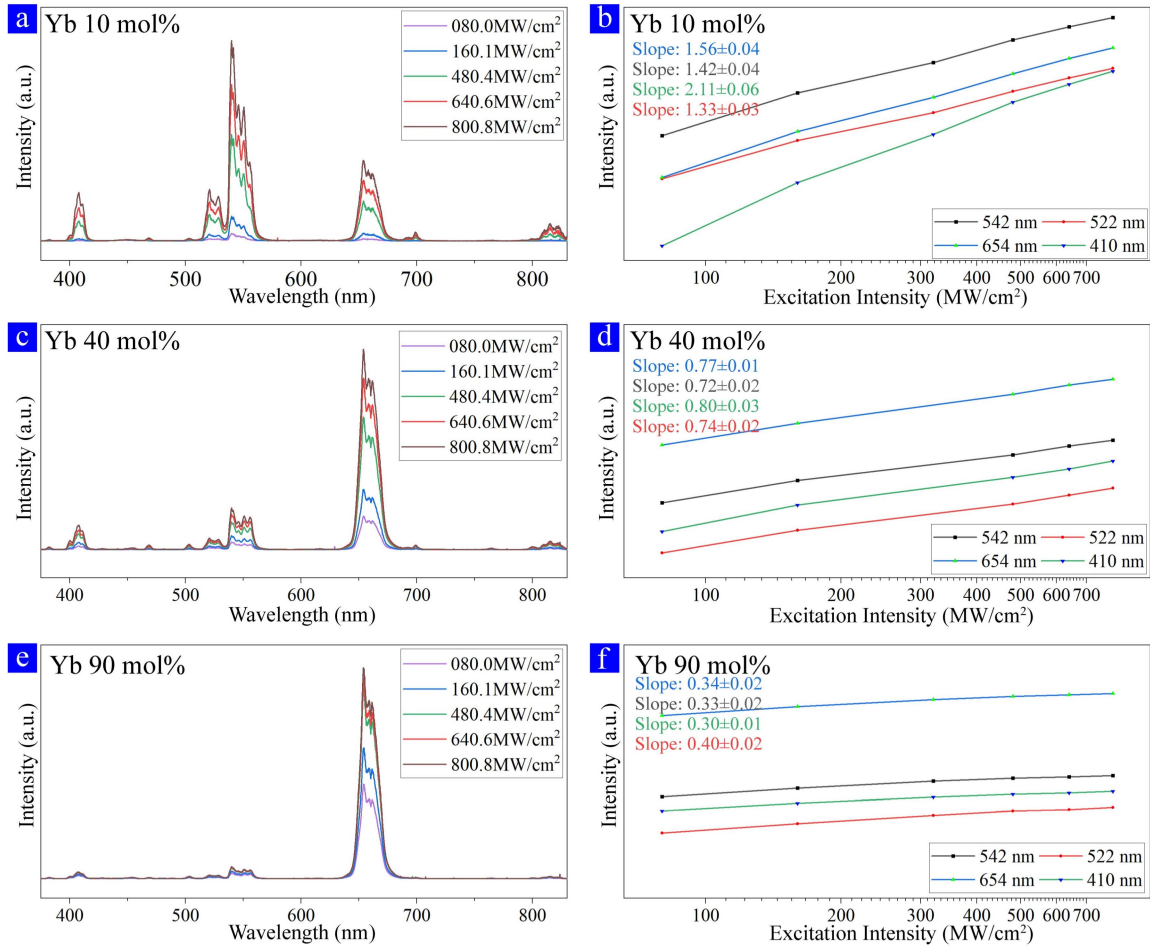


Figure S1 (a), (c), and (e) Power-dependent UCL spectra of a single β -NaY(Yb)F₄: Yb/Er ($x/2$ mol%) MCs in the 375 to 830 nm regions under the excitation of 976 nm ns-pulsed laser. (b), (d), and (f) The dependence of the UC emission intensity on the excitation intensity for a single β -NaY(Yb)F₄: Yb/Er ($y/2$ mol%) MCs with different UC emission bands.

In addition, we have also measured the power-dependent UCL spectra and power efficiency under the excitation of continuous-wave (CW) lasers, as shown in Figure S2. Unlike the ns-pulsed excitation, significant multiband emission phenomena can be more obviously observed under CW laser excitations. Although the irradiation power density of ns-pulsed laser excitation is two orders of magnitude greater than that of CW laser excitation, the excitation duration of ns-pulsed laser is only ~15 ns. As the result, the single MCs only absorbs photons in a very short period of time and produces a short-lived multiband emissions. It makes the power efficiency under ns-pulsed excitation higher than CW excitation. However, at the same time, the energy loss rate of individual MC increases due to the energy migration of Yb-Yb ions.^{2, 3} The effect of Yb-Yb migration makes the power efficiency lower with increasing the doping concentration under ns-pulsed excitation.

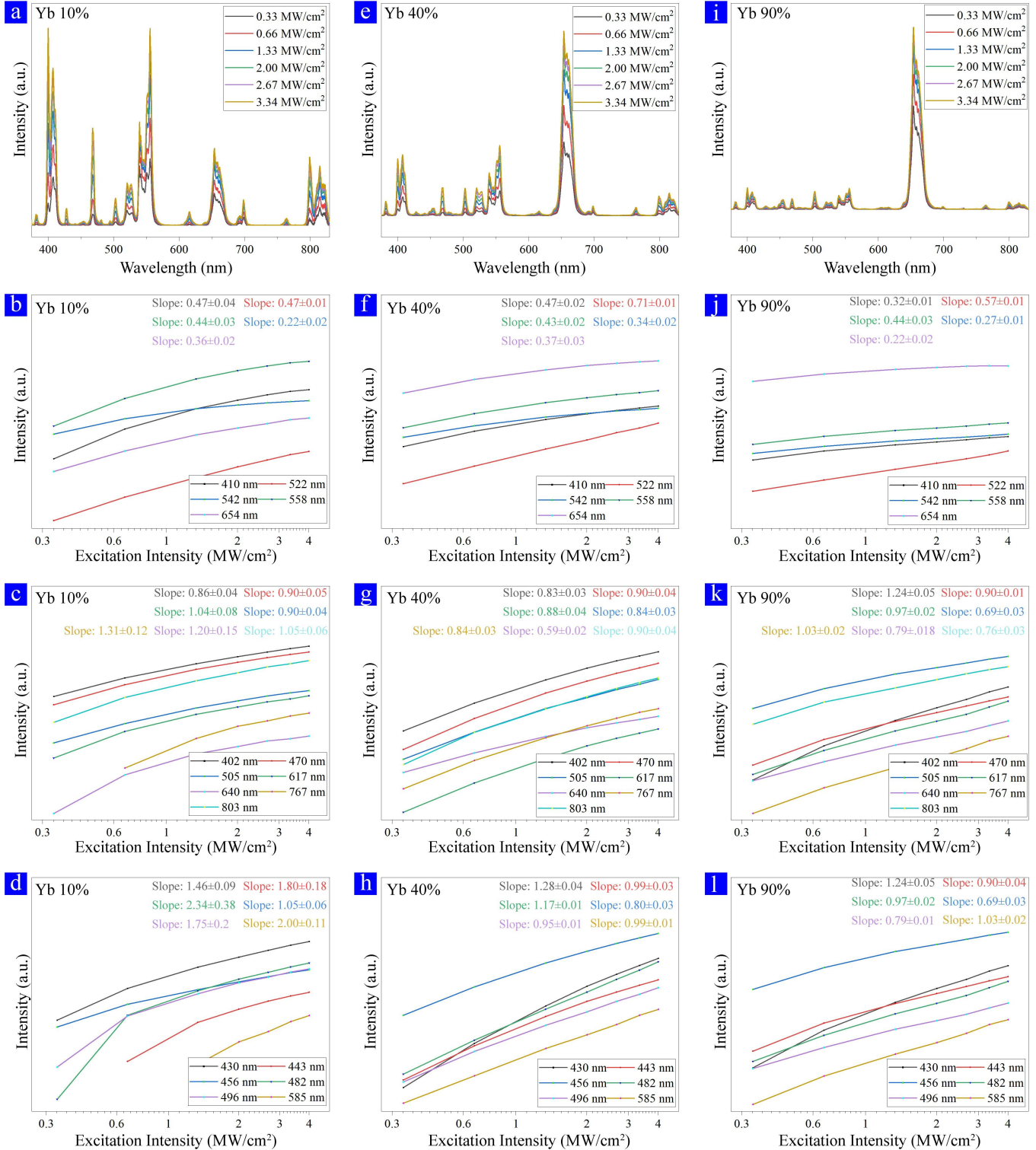


Figure S2 (a), (e), and (i) P-dependent UCL spectra of a single β -NaY(Yb)F₄: Yb/Er ($x/2$ mol%) MC in the 375 to 830 nm wavelength region by excitation of a 976nm CW laser. (b-d), (f-h), and (j-l) The dependence of the UC emission intensity on the excitation intensity of a CW laser for a single β -NaY(Yb)F₄: Yb/Er ($y/2$ mol%) MC with different UC emission bands.

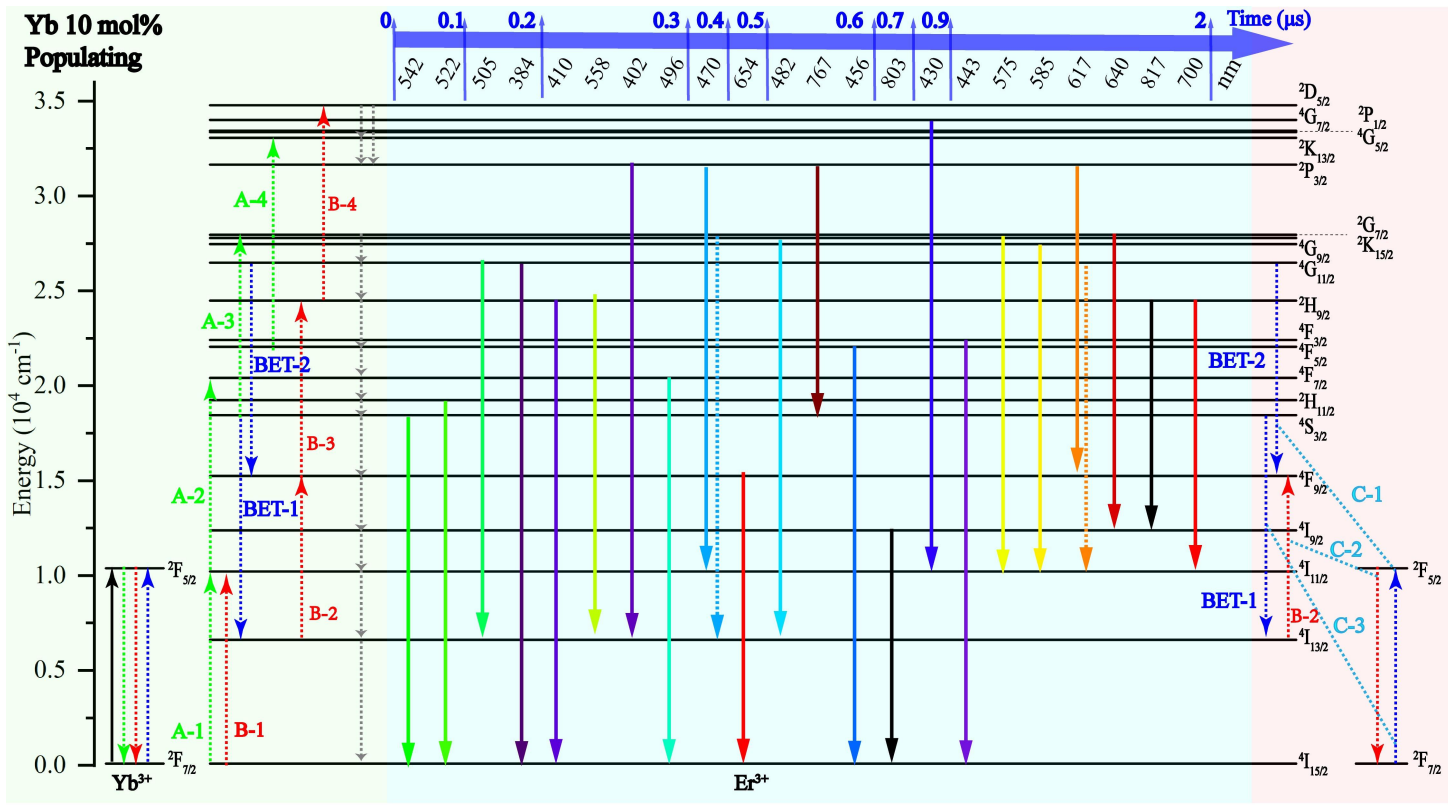


Figure S3 Schematic representation of the transition kinetics on the first 2 μ s after the 976 nm ns-pulsed excitation in NaYF₄:Yb/Er (10/2 mol%). The green part shows the process of establishing electron populations and the nRP. The blue part shows the all radiative transition of multiband UCL.

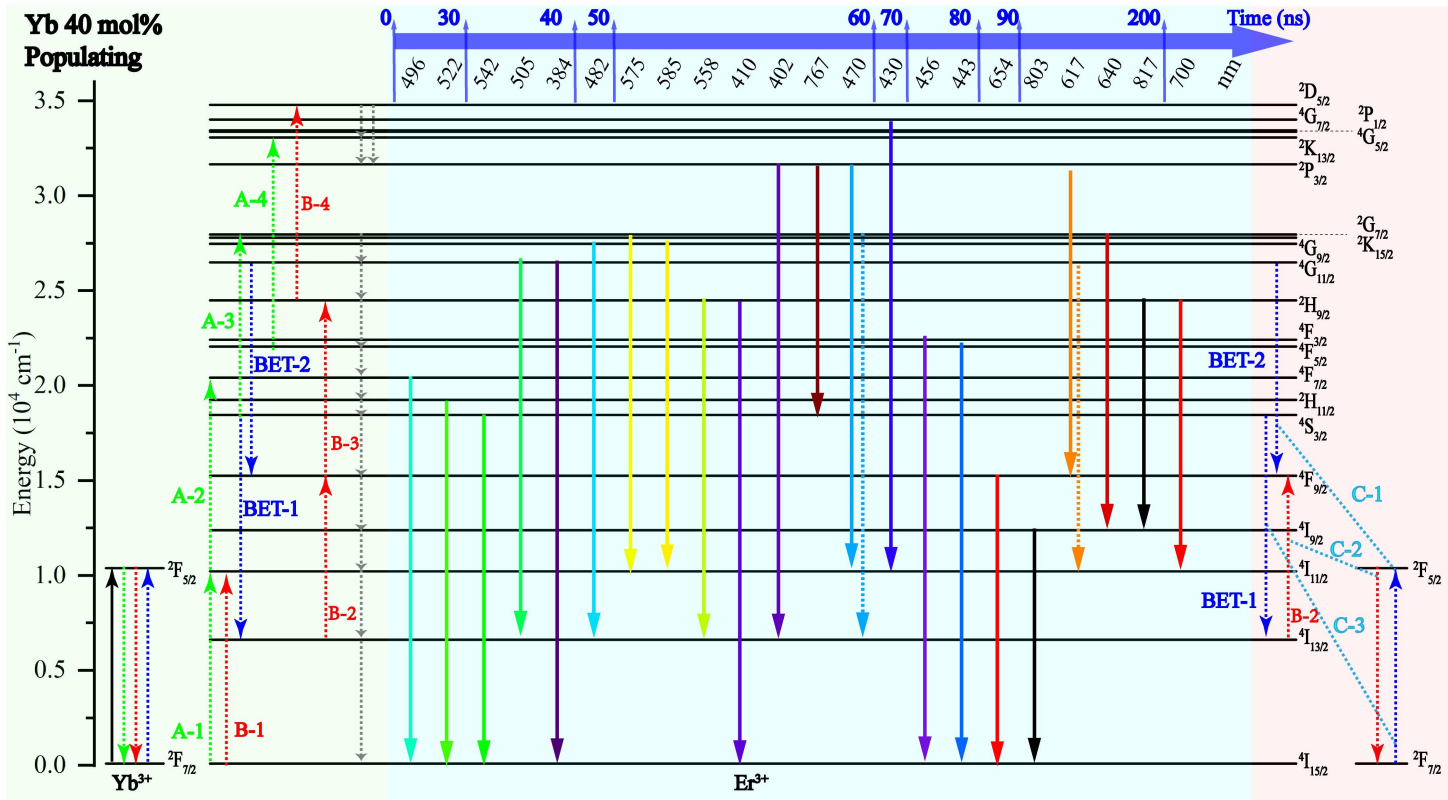


Figure S4 Schematic representation of the transition kinetics on the first 2 μ s after the 976 nm ns-pulsed excitation in NaYF₄:Yb/Er (40/2 mol%). The green part shows the process of establishing electron populations and the nRP. The blue part shows the all radiative transition of multiband UCL.

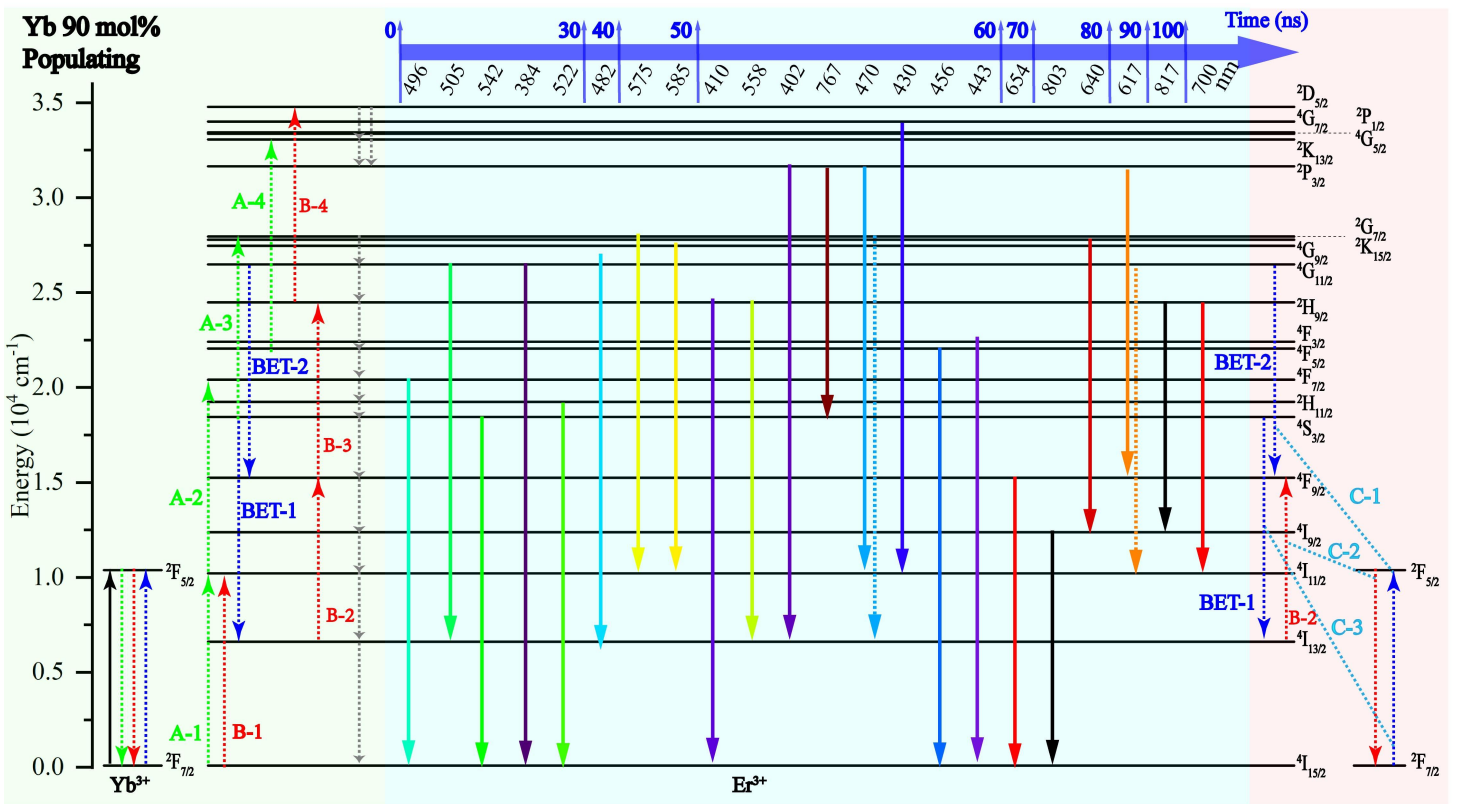


Figure S5 Schematic representation of the transition kinetics on the first 2 μ s after the 976 nm ns-pulsed excitation in NaYF₄:Yb/Er (90/2 mol%). The green part shows the process of establishing electron populations and the nRP. The blue part shows the all radiative transition of multiband UCL.

We have further measured the luminescence properties for the β -NaYbF₄:Er³⁺ and compared with the relatively lower Yb³⁺ concentrations MCs. As shown in Figure S6, XRD and SEM results show that the size and crystalline phase of the β -NaYF₄:Er (2 mol%) and NaY(Yb)F₄:Yb/Er (90/2 mol%) MCs are similar. The luminescence spectra and evolution spectrum after ns-pulsed excitation of these two kinds of MCs exhibit the same variation trends, as shown in Figure S7. Then, we further analyze the transition kinetics of β -NaYF₄:Er (2 mol%) and NaY(Yb)F₄:Yb/Er (90/2 mol%) MCs (Figure S8). The same results can be observed for these two MCs. There is no obviously different.

Furthermore, we calculated the CIE chromaticity coordinates and the multiband UCL lifetimes, as shown in Figure S9. It finds that the β -NaYF₄:Er (2 mol%) MC moves faster towards red emission compared to NaY(Yb)F₄:Yb/Er (90/2 mol%) MCs. The reason is the increase in the proportion of red emission (654 nm) and the decay rate of other UCL as the C-1,C-2,C-3 process (see Figure S8) intensifies with the increase in Yb³⁺ concentrations. The multiband emissions lifetime of β -NaYF₄:Er (2 mol%) MCs is slightly smaller than that of NaY(Yb)F₄:Yb/Er (90/2 mol%) MC. This is due to the surface leakage of energy caused by the migration of Yb-Yb as the Yb³⁺ concentration increases.² In addition, we have also analyzed the populating process for the β -NaYbF₄:Er (2 mol%) and β -NaY(Yb)F₄:Yb/Er (90/2 mol%) MCs. The rising rate of β -NaYbF₄:Er (2 mol%) MC is a little bit faster than β -NaY(Yb)F₄:Yb/Er (90/2 mol%) MCs.

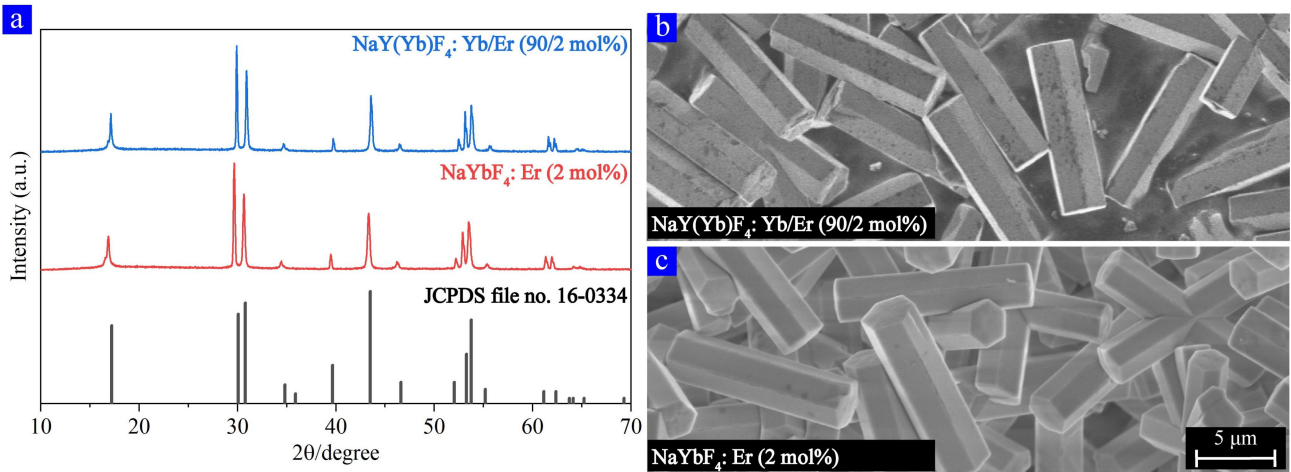


Figure S6 (a) XRD patterns of the as-prepared $\beta\text{-NaY(Yb)F}_4$: Yb/Er (90/2 mol%) and $\beta\text{-NaYbF}_4$: Er (2 mol%) MCs compared to the known peaks of the hexagonal phase of NaYF_4 . SEM micrographs of (b-c) $\beta\text{-NaY(Yb)F}_4$: Yb/Er (90/2 mol%) MCs and $\beta\text{-NaYbF}_4$: Er (2 mol%) MCs.

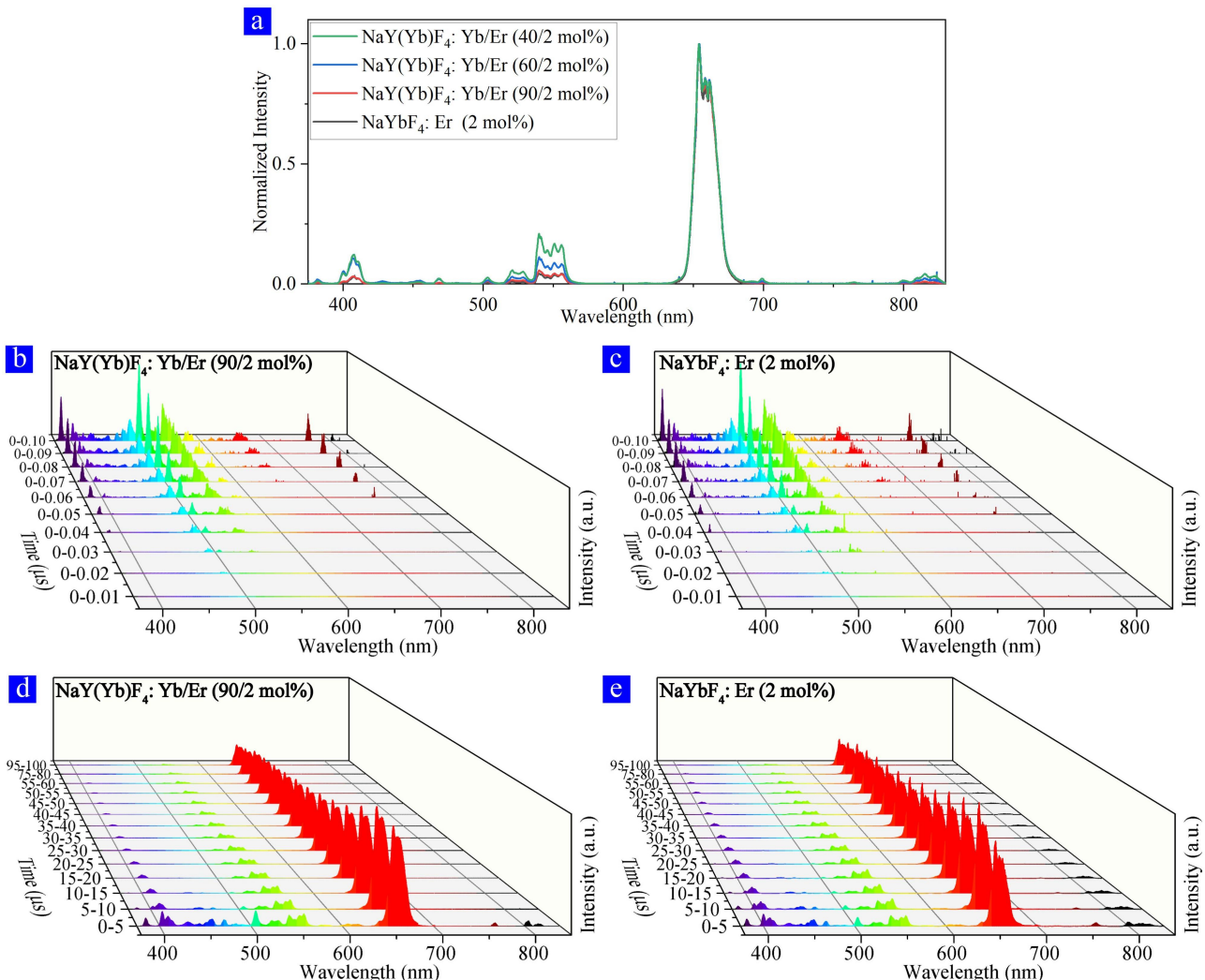


Figure S7 (a) Spectrum of individual MC emitting total UCL (range from 375 nm to 830 nm) after each ns-pulse excitation. The 0 moment is the starting point of the 976 nm ns-pulsed excitation. Time evolution spectrum of (b,d) $\beta\text{-NaY(Yb)F}_4$: Yb/Er (90/2 mol%) MC and (c,e) $\beta\text{-NaYbF}_4$: Er (2 mol%) MC measured by superimposed transient spectrum at the same moment.

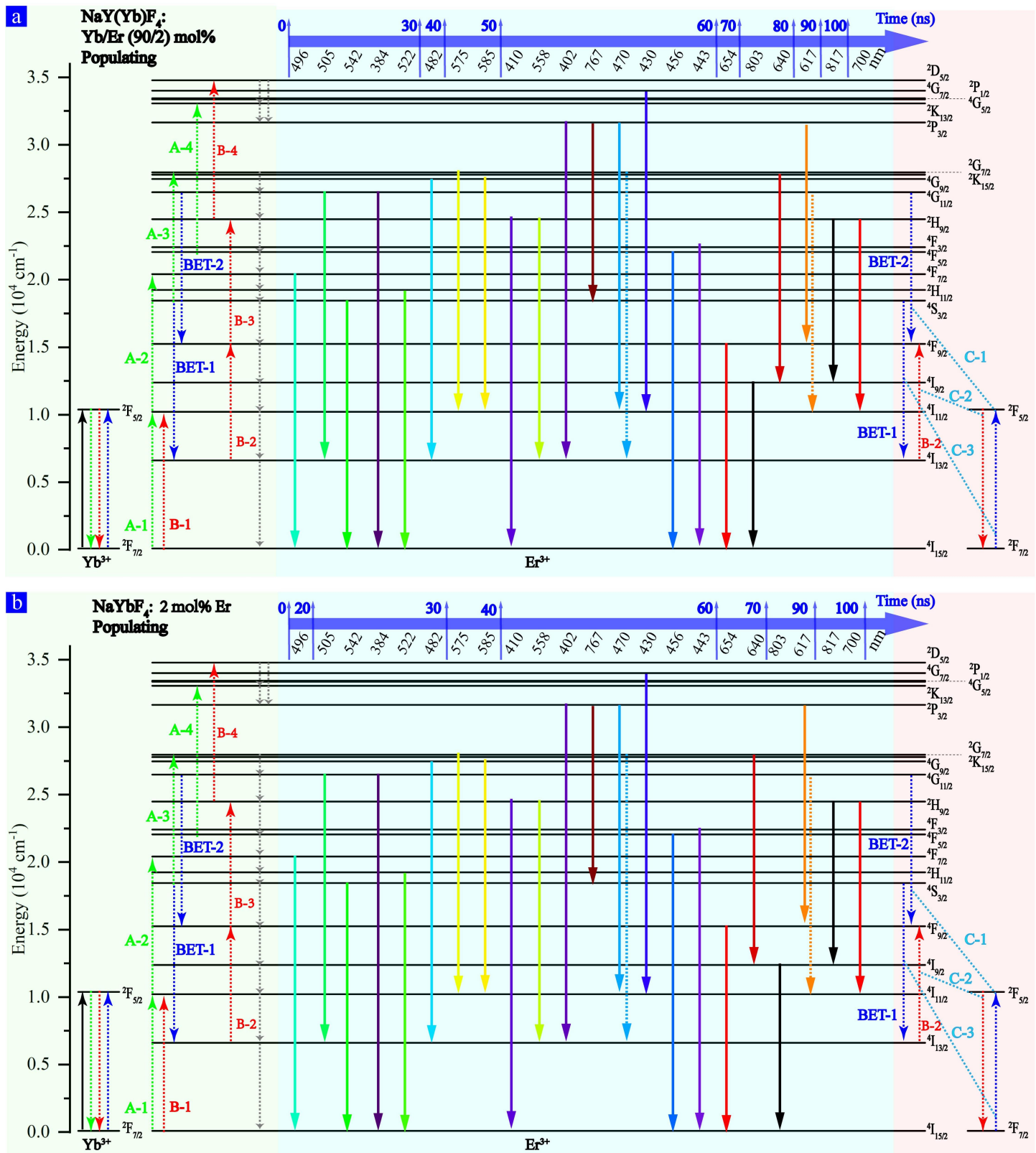


Figure S8 Schematic representation of the transition kinetics on the first 100 ns after the 976 nm ns-pulsed excitation in $\beta\text{-NaY}(\text{Yb})\text{F}_4$: Yb/Er (90/2 mol%) MC and $\beta\text{-NaYbF}_4$: Er (2 mol%) MC. The green part shows the process of establishing electron populations and the nRP. The blue part shows the all radiative transition of multiband UCL. The red part shows the main populating process of red emission enhancement.

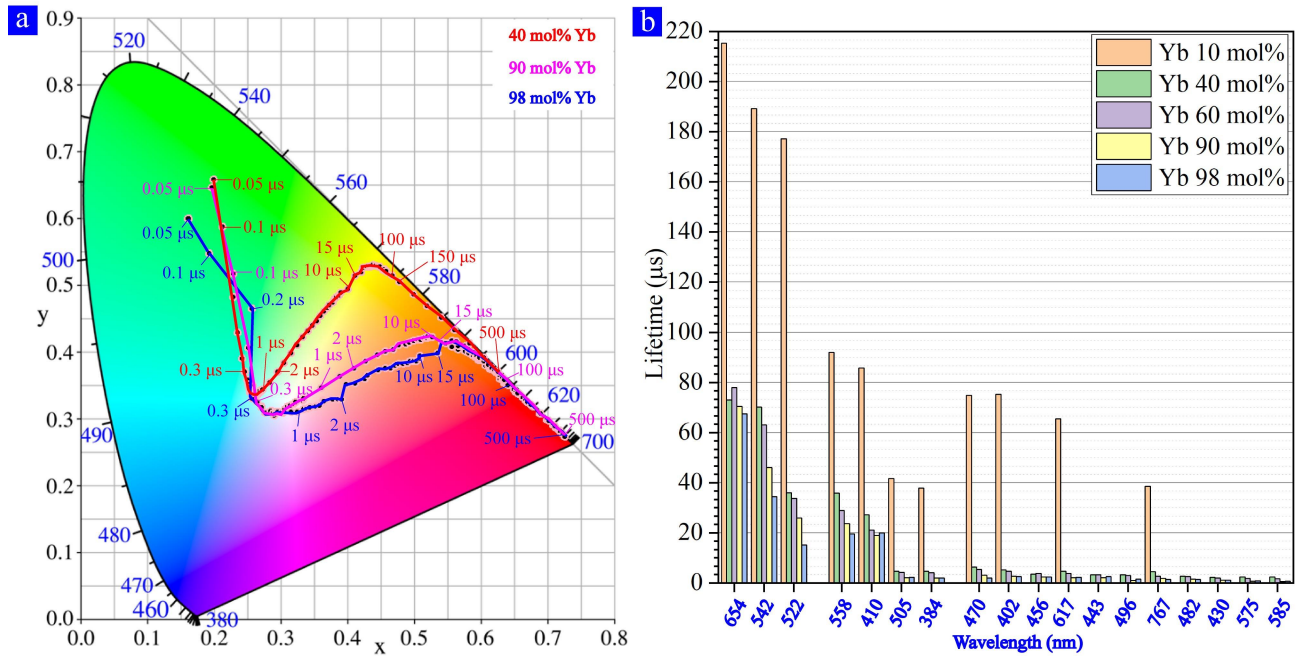


Figure S9 The 0 moment is the starting point of the 976 nm ns-pulsed excitation. (a) CIE chromaticity coordinates for the multiband UCL of the single β -NaY(Yb)F₄:Yb/Er MC with different Yb³⁺ concentrations and β -NaYbF₄: Er (2 mol%) MC. (b) The multiband UCL lifetimes of single β -NaY(Yb)F₄:Yb/Er MC with different Yb doping concentrations and β -NaYbF₄: Er (2 mol%) MC.

Reference

1. M. Pollnau, D. R. Gamelin, S. R. Lüthi, H. U. Güdel and M. P. Hehlen, *Phys. Rev. B*, 2000, **61**, 3337–3346.
2. B. Shen, S. Cheng, Y. Gu, D. Ni, Y. Gao, Q. Su, W. Feng and F. Li, *Nanoscale*, 2017, **9**, 1964–1971.
3. R. Arppe, I. Hyppänen, N. Perälä, R. Peltomaa, M. Kaiser, C. Würth, S. Christ, U. Resch-Genger, M. Schäferling and T. Soukka, *Nanoscale*, 2015, **7**, 11746–11757.